Kinetic Studies by Fluorescence Resonance Energy Transfer Employing a Double-Labeled Oligonucleotide: Hybridization to the Oligonucleotide Complement and to Single-Stranded DNA†

Kay M. Parkhurst and Lawrence J. Parkhurst*

Department of Chemistry, University of Nebraska—Lincoln, Lincoln, Nebraska 68588-0304

Received July 19, 1994; Revised Manuscript Received October 14, 1994®

ABSTRACT: A single 16-base oligodeoxyribonucleotide was labeled at the 3′-end with fluorescein and at the 5′-end with x-rhodamine (^{R*}oligo^{*F}); the chromophores served as a donor/acceptor pair, respectively, for Förster resonance energy transfer. We exploited the striking differences in the steady-state emission spectra of the ^{R*}oligo^{*F} as a single strand and in a duplex structure to signal hybridization in solution and to determine the kinetics of duplex formation as the probe bound to its oligomer complement and to its target sequence in M13mp18(+) phage DNA. The binding followed second-order kinetics; in 0.18 M NaCl (pH 8) with 25% formamide, the rate constant for binding to the oligomer complement was 5.7×10^5 M^{-1} s^{-1}, and that to M13mp18(+) was 5.7×10^4 M^{-1} s^{-1}. The source of the 10-fold decrease in the rate of binding to M13mp18(+) was examined to differentiate between multiple nonproductive nucleation and rapid fluctuations in the structure around the target site. From simulations based on each model combined with associated experimental results, we concluded that the slower binding was due to rapid structural fluctuations around the target site, with an effective target concentration 0.1 of that of the total. Comparisons of total fluorescein emission derived from both steady-state and lifetime measurements suggest that the 5′-x-rhodamine induces a conformational change that affects the interaction at the 3′-end between the fluorescein and the polymer. The effects of salt on the fluorescence were complex. The static quenching of fluorescein in the single-labeled, single-stranded oligonucleotide did not change with NaCl (0−0.18 M), whereas there were marked changes in the double-labeled probe, showing that the conformational effects mediated by the 5′-x-rhodamine were salt dependent.

Over the past decade, oligonucleotides have been modified in a variety of ways to be used as probes for detecting hybridization. These modifications have included incorporation of a radioactive label, binding of a substrate such as biotin, binding of an enzyme such as alkaline phosphatase [a review of these probes can be found in Tenover (1989)], or binding of spectroscopic labels (Cardullo et al., 1988; Morrison et al., 1989; Heller & Morrison, 1985; Cooper & Hagerman, 1990). In the latter, fluorophores were bound covalently to either the 3′- or 5′-end of DNA oligomers, with nonradiative transfer of the excitation energy or quenching of fluorescence in response to hybridization. These studies have utilized, in various ways, one or more single-labeled oligomers. We were interested in exploiting the potential of a double-labeled oligomeric strand for the detection of hybridization in solution and for monitoring binding in real time, for use both as a DNA probe and as a tool for examining the physical behavior of oligomers in solution. Our study utilized a 16-mer oligodeoxyribonucleotide labeled at the 3′-end with fluorescein and at the 5′-end with x-rhodamine and was based on assumed different efficiencies of Förster energy transfer for the unhybridized probes. We report here the use of the probe to signal hybridization in solution and to determine the kinetics of duplex formation as the probe hybridized to its complementary oligomer and to its target sequence in M13mp18(+) phage DNA.

Resonance interaction between two chromophores allows the direct transfer of excitation energy from the donor to the acceptor chromophore, and the rate of transfer for such weak coupling varies with the inverse sixth power of the distance between the two moieties. Our initial conceptual model for the single-stranded oligomer in solution was that of a random coil, with the ends of the coil, on the average, sufficiently close together to allow efficient energy transfer. Since 16 base pairs correspond to 1.5 turns of a double helix, the two fluorophores would be positioned on opposite sides of the helix when the labeled 16-mer hybridized to its complement, giving a large separation between donor and acceptor and a low efficiency of energy transfer. The relative emission spectra of the donor and the acceptor would be expected to reflect this difference in their distance apart. The donor/acceptor pair fluorescein/x-rhodamine has a Förster distance R_0 (the distance at which transfer is 50% efficient) of 59.6 Å, which is well suited to the distance between the terminal 3′- and 5′-oxygens in one strand of a 16-mer duplex, 54.7 Å (Insight II, Biosym Technologies, San Diego, CA). The sequence of the oligomer (5′-GTAAAACGACGGCCAG-3′) is complementary to bases 6291−6306 on M13mp18(+), adjacent but one to the restriction site, and has no self-complementarity.

When fluorescein was excited near its absorbance maximum, the emission spectra of both donor and acceptor clearly

† This work was supported by National Institutes of Health Research Grant DK 36288 and by grants from the Center for Biotechnology, University of Nebraska—Lincoln.

* Author to whom correspondence should be addressed. Telephone: (402) 472-3316. e-mail: lparkhurst@unl.edu. FAX: (402) 472-9402.

® Abstract published in *Advance ACS Abstracts,* December 1, 1994.

0006-2960/95/0434-285$09.00/0

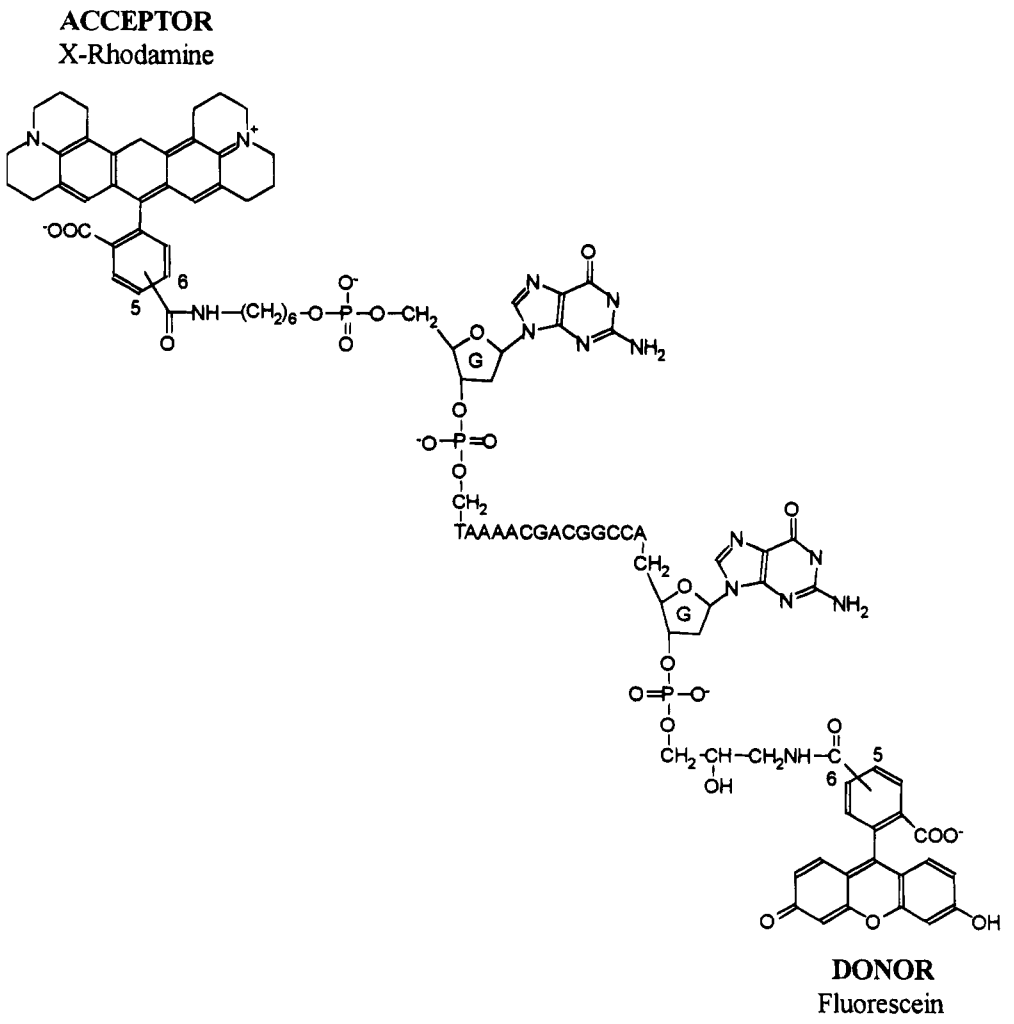

FIGURE 1: Fluorescent double-labeled probe: a 16-base oligodeoxyribonucleotide with x-rhodamine bound to the 5′-end and fluorescein bound to the 3′-end. The fluorescein and x-rhodamine serve as a donor/acceptor pair, respectively, for Förster energy transfer. The efficiency of transfer is very sensitive to the distance separating the two fluorophores and to the flexibility of the polymer.

reflected the transition from random coil to duplex and the change could be monitored simply in real time, allowing direct measurement of the kinetics of hybridization (Parkhurst & Parkhurst, 1992, 1993). It became clear from kinetic analysis that the rate constant for the oligomer binding to M13mp18(+) was much slower than that for hybridization to the 16-mer complement. Since the association kinetics appeared to follow second-order kinetics, it was reasonable to analyze the results in terms of rapid equilibria preceding the binding of the probe. We therefore examined the source of the reduced binding rate to differentiate between multiple nonproductive nucleation and rapid fluctuations in structure around the binding site. In order to understand the various changes in the steady-state fluorescence spectra of these species, it was necessary to construct an optical cycle and incorporate information from lifetime measurements.

EXPERIMENTAL PROCEDURES

Tris-HCl was purchased from Sigma (St. Louis, MO). Formamide, from Sigma, was deionized prior to use by passing it over a column containing Chelex 100 biotechnology grade chelating resin (from Bio-Rad Laboratories, Richmond, CA) and then stored at −80 °C. The 16-mer deoxyribonucleotide with a 5′-x-rhodamine and a 3′-fluorescein (^{R*}oligo^{*F};[1] Figure 1) was synthesized and HPLC-purified by Research Genetics, Inc. (Huntsville, AL). Also purchased were the single-labeled oligomers with only 5′-x-rhodamine (^{R*}oligo) and only 3′-fluorescein (oligo^{*F}). The 16-mer complement (oligo$_{16c}$) to this oligomer and the 16-mer identical to the probe but without the fluoresphores (^{0}oligo^{0}) were synthesized in our departmental oligonucleotide synthesis facility and shown to be >95% pure by gel electrophoresis. The circular phage DNA M13mp18, both single- and double-stranded, was purchased from Sigma.

Instrumentation and Data Analysis. Absorbance spectra were collected on a Hewlett-Packard diode array spectrophotometer (Model HP8452A). The steady-state fluorescence measurements were made using a fluorimeter (Photon Technology International, Inc., Model A-1010) with computerized data acquisition and modified to use an argon ion laser (Lexel, Model 75) as the excitation light source at 488 nm. The laser output was set so that 6 mW was the power incident on the sample. Fluorescence emission spectra were collected and smoothed using PTI software: 500−625 nm

[1] Abbreviations: all oligonucleotides are oligodeoxyribonucleotides; ^{R*}oligo^{*F}, the 16-base oligomer 5′-GTAAAACTGACGGCCAG-3′ with x-rhodamine (structure shown in Figure 1) covalently bound at the 5′-end and fluorescein at the 3′-end; oligo^{*F}, the 16-base oligomer with only 3′-fluorescein; ^{R*}oligo, the 16-base oligomer with only 5′-x-rhodamine; ^{0}oligo^{0}, the 16-base oligomer with no fluorescent labels; oligo$_{16c}$, the 16-base complement to the oligomer.

for ^{R*}oligo^{*F}, 550−550 nm for oligo^{*F}, and 590−630 nm for ^{R*}oligo. Oligomer concentrations ranged from 1.5 to 25 nM in a solution volume of 250 μL in a short microcuvette (2 mm wide × 10 mm (parallel to laser beam) × 20 mm high). The rhodamine reference cell (quantum counter) built into the fluorimeter was used in all cases requiring a series of related measurements to correct for fluctuations in the intensity of the excitation beam. A Lauda K-2/R constant-temperature circulating bath was used to thermostat the cuvette holder.

Fluorescence lifetime measurements were made in the frequency domain on an SLM-Aminco 4850 Multi Harmonic Frequency spectrofluorometer as follows: phase shift and modulation data were obtained simultaneously over 30 frequencies, with a base frequency of 5 MHz, and with a 520 nm interference filter (Oriel Corp., Stratford, CT) positioned between the sample and the photomultiplier. For each measurement, three consecutive scans were collected and averaged. Four or five such data sets were averaged to make a composite file, which was fit to both single- and biexponential models. The SLM-Aminco software was used to find the best-fitting τ's and preexponential terms, minimizing the weighted sums (over frequency) of squared residuals for the observed and calculated phase shift and modulation vectors. Lifetime measurements were made on the oligo^{*F} and on the ^{R*}oligo^{*F}, both as single strands and in a duplex structure with the 16-mer complement. The oligomer concentration ranged from 140 to 380 nM, and measurements were made at ambient temperature (20−22 °C).

Characterization of the Double- and Single-Labeled Oligomers. Both steady-state and lifetime measurements were made on each of the following four materials (A−D) to better understand changes in the fluorescein emission (represented by the arrows):

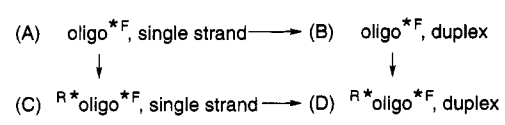

The steady-state ratios of B/A and D/C were obtained by scanning 2.5 nM A and C from 500 to 625 nm and then adding a 2−3-fold excess of oligo$_{16c}$ and scanning again 30 min after hybridization was complete. The steady-state ratios of C/A and D/B were obtained by direct comparison of the peak emission intensities for identical concentrations of each material. By comparing the steady-state and integrated lifetime ($\int I_F(t)\,dt$) ratios, the extent of static quenching could be determined for any given pair.

The lifetime measurements were obtained, as described previously, on 380 nM solutions of ^{R*}oligo^{*F} and 140 nM solutions of oligo^{*F}. Because of the higher concentrations, it was reasonable to consider the possibility of polymerization. Dye stacking would result in changes in the absorbance spectrum due to exciton interactions; spectra therefore were obtained on 4−5 μM solutions of ^{R*}oligo^{*F}, oligo^{*F}, and ^{R*}oligo from 240 to 700 nm.

The effect of [NaCl], from 0 to 0.18 M, on the emission of the bound fluorescein was investigated for single strands of oligo^{*F} and ^{R*}oligo^{*F}. For oligo^{*F}, only steady-state measurements were made; for ^{R*}oligo^{*F}, both steady-state and lifetime measurements were made. In each case, the NaCl concentrations were 0, 0.023, 0.066, 0.107, and 0.18 M, achieved by making successive 2−4% volume additions of 1.18 M NaCl to the initial solutions and correcting the steady-state emission scans for dilution. The initial concentration of oligo^{*F} was 8 nM. The concentrations of ^{R*}oligo^{*F} for the steady-state measurements and the lifetime measurements were 10 and 350 nM, respectively.

In 0.01 M Tris (pH 8) with 0.18 M NaCl, the fluorescein/x-rhodamine peak ratio for the ^{R*}oligo^{*F} as a single strand and in a duplex structure differed in the presence and absence of formamide. To understand the source of this difference, the fluorescein and/or x-rhodamine emission of each of the oligomers A−D in the scheme above, as well as of the ^{R*}oligo as a single strand and in a duplex, was measured with and without 25% formamide. An initial measurement was made on 250 μL of 3−6 nM of each material, and then 85 μL of formamide and 15 μL of 1.18 M NaCl (to maintain the salt concentration at 0.18 M) were added, a scan was taken, and the peak emission intensity was corrected for the dilution.

Demonstration of Hybridization and Kinetic Measurements. For the experiments to detect hybridization, the buffers were 0.01 M Tris (pH 8), 1 mM EDTA, and 0.18 M NaCl, both with and without 25% formamide. Solutions containing oligo$_{16c}$, M13mp18(+), M13mp18-RF, or 25% formamide showed measurable background fluorescence between 500 and 625 nm and/or Raman scattering from water with a peak at 583 nm (17 153 cm^{-1}). The solution with the target DNA sequence was therefore scanned for a baseline spectrum, which was substracted from each subsequent scan prior to data analysis. Following the baseline scan, the ^{R*}oligo^{*F} was added, mixed, and, for collection of kinetic data, the initial scan was taken 0.5 min from the time of addition; for static measurements, several scans were taken when hybridization was complete to ensure than an end point had been reached.

The duplex structure composed of ^{R*}oligo^{*F} and oligo$_{16c}$ was formed following the procedure described earlier of adding 10−35 μL of ^{R*}oligo^{*F} (to a final concentration of 1.5−3 nM) to 250 μL of 2−12 nM oligo$_{16c}$, at ambient temperature (20−22 °C). For kinetic experiments, scans were taken every 0.5−5 min for 30 min, with stirring after each scan. Controls with ^{R*}oligo^{*F} only showed that this procedure produced scans that could be superimposed; the laser beam probes approximately 0.15 of the total volume of the solution, and the effect of bleaching became negligible when the volume of solution exposed to the laser beam was mixed with the total volume following each scan.

Hybridization of the probe to M13mp18(+) and determination of the associated kinetics were carried out in two ways. One method was to add 2.8 nM ^{R*}oligo^{*F} to 5.6−11.2 nM M13mp18(+) in the 25% formamide solution and scan from 500 to 625 nm. The solution was mixed and subsequent scans were collected every 1.5−5 min for 30 min and then every 10−20 min for 4 h, mixing after each scan, until hybridization was complete, as indicated by multiple scans with a constant fluorescein/x-rhodamine peak ratio. Alternatively, ^{R*}oligo^{*F} was added to M13mp18(+) and scans were taken as before for 45 min. The solution was incubated for 2 min at 65 °C in a heat block (Thermolyne, Model 17600) and cooled to ambient temperature over 30 min. A final scan was taken and repeated in 5 and 10 min to ensure that an end point in the hybridization reaction had been reached. When a control, with just ^{R*}oligo^{*F} and no

M13mp18(+) in the solution, was subjected to this procedure, the final and initial scans were superimposable, confirming that the heating, cooling, and concurrent pH changes in the Tris buffer ultimately did not affect the emission of the conjugated labels. In the absence of formamide, this hybridization reaction was observable but was very slow, with the ratio of fluorescein/x-rhodamine only changing from 0.45 to 0.47 in 150 min. After 150 min, the solution was incubated for 2 min at 65 °C in a heat block, cooled to ambient temperature over 30 min, and scanned. It was again heated to 65 °C for 2 min, immediately put on ice, and then returned to ambient temperature and scanned. These two heating and cooling cycles were repeated several times on the same solution.

The double-stranded M13mp18-RF was denatured prior to hybridization by subjecting the solution to a boiling water bath for 2 min and cooling on ice; the solution was returned to ambient temperature and a baseline scan was taken. To 2 nM M13mp18-RF was then added 1.5 nM ^{R*}oligo^{*F}, the initial scan was taken, and the solution was placed in a 95 °C heat block for 2 min. The solution was returned to ambient temperature over 30 min and a second scan was taken. The solution was left at ambient temperature and scanned at 24 and at 48 h. A control of ^{R*}oligo^{*F} alone, subjected to an identical procedure, showed minimal change in the 500−625 nm scan. This procedure was done with and without 25% formamide.

Investigation of the 10-fold Difference in Rate Constants for ^{R*}Oligo^{*F} Binding to Complement vs Binding to M13mp18(+). The association constant for the probe hybridizing to M13mp18(+) was an order of magnitude lower than the rate constant measured for the probe hybridizing to the 16-mer complement. This difference could derive from structural fluctuations at or near the target sequence that rendered the target sequence inaccessible, effectively decreasing the target site concentration to 0.1 of that of the total. It could also be the consequence of multiple nucleation complexes formed by the probe with nontarget sites on the M13, which would effectively decrease the concentration of probe. A simulation and a series of experiments were performed to examine the source of this kinetic difference.

A computer search showed the 16-mer probe sequence to have only one target site on M13mp18(+), and the sequence remained unique for up to five base-pairing mismatches. When six or more random mismatches were allowed, multiple target sites were identified. Truncation of six or more bases from either the 5′- or 3′-end of the probe also resulted in sequences with multiple sites on M13mp18(+). A simple model for multiple nucleation was adopted having n nucleation sites (1 target site and $n - 1$ nonproductive sites), each nontarget site with the same binding constant, K, for the probe, and assuming rapid equilibration between probe and nucleation site relative to that for hybridization between probe and target site. Consider the following equations:

$$D_1 + P \xrightarrow{k_1} D_1P \quad (1)$$

$$D_nP_i + P \rightleftharpoons D_nP_{i+1} \quad (2)$$

where eq 1 describes hybridization of the probe, P, to the target sequence, D_1, and eq 2 describes one step of multiple binding, with an association constant K, of probe to any of n nontarget sites, with $i = 0-(n-1)$. At any time, the total probe concentration potentially available for target hybridization, $[P_T']$, is total probe, $[P_T]$, minus probe already hybridized to target, $[D_1P]$, and can be written as a sum of free probe, [P], plus probe involved in nonproductive nucleation:

$$[P_T] - [D_1P] = [P_T'] = [P] + \frac{nK[P][D_T]}{1 + K[P]} \quad (3)$$

where $[D_T]$ is total M13mp18(+).

For the simulation, $[P_T]$ and $[D_T]$ were assigned values of 1 and 1.5 nM, respectively. At time $t = 0$, $[D_1P] = 0$ and $[P_T'] = [P_T]$. Simple numerical integration was used to obtain the change in $[D_1P]$ at each time increment for $t > 0$, using $\Delta[D_1P] = k_1[D_1][P](\Delta t)$, with [P] from eq 3, $[D_1] = [D_T] - [D_1P]$, and k_1 assigned the value 1×10^5 M^{-1} s^{-1}, which is approximately the value of the second-order rate constant measured for the probe binding to the 16-mer complement. The half-time of the reaction occurred when $[P_T'] = [P_T]/2$, and the apparent rate constant for the hybridization reaction, k_2, was determined directly from $t_{1/2}$. The number of sites, n, was varied from 1 to 100. For each value of n, K in eq 3 was varied until the value calculated from k_2 was 1×10^4 M^{-1} s^{-1}, to agree with the observed value (k') of $k_1/0.1$. Seven (n,K) pairs that were consistent with the measured rate constants were thus identified. The dependence of k_1 on [M13mp18(+)] was determined by running the simulation again, with $[P_T] = 1$ nM but $[D_T]$ increased by 4-fold to 6 nM. The value of k_2 was determined for each of the seven (n,K) pairs obtained previously. The results showed a marked concentration dependence of k_2 on $[D_T]$, with k_2 *decreasing* 3.7−5 times for the seven (n,K) pairs in response to a 4-fold *increase* in $[D_T]$.

If the lower rate constant for probe binding M13mp18(+) were due to equilibria among secondary or tertiary structures around the target sequence, the hybridization reaction could be described simply as

$$D_1 \rightleftharpoons D_i \quad (4)$$

$$D_1 + P \xrightarrow{k_1} D_1P \quad (5)$$

where D_1 is DNA with an accessible target sequence, D_i is any form of the DNA with the target rendered inaccessible due to structural fluctuations, K_i is the associated equilibrium constant, and k_1 is the rate constant for the formation of product, D_1P. Then $d[D_1P]/dt = k_1[D_1][P]$, but $[D_1] = \phi[D_T]$, where $\phi = 1/(1 + \Sigma K_i)$ and where, again, the equilibria in eq 4 are assumed to be established rapidly with respect to the kinetics in eq 5. The observed rate constant, k', equals ϕk_1 and is independent of the concentration of M13mp18(+). The rate constant k_1 is assumed to be that for the probe binding to the oligo$_{16c}$ complement.

Having established the *dependence* of k on the M13mp18(+) concentration for the multiple nucleation model and the *independence* of k' from [M13mp18(+)] for the structural fluctuation model, we designed a series of experiments to examine directly the effect of various concentration changes on k'. In all of these experiments, the solution contained 25% formamide and 0.18 M NaCl. An oligomer (^{0}oligo^0) was prepared having the same

sequence as the probe, but with no bound fluorescein or x-rhodamine. This oligomer was used to block the target sequence in M13mp18(+) by incubating it in various mole ratios relative to M13mp18(+) for 3 h (to essentially complete hybridization) prior to the monitored hybridization reaction with the labeled oligomer. In this way, potential nucleation sites could be varied independently of the target concentration. Hybridization of the product with ^{R*}oligo^{*F} was monitored and analyzed as described previously for kinetic experiments.

To confirm the effectiveness of the unlabeled probe in blocking the target sequence, ^{0}oligo^{0} was used first with the 16-mer complement, as follows: 3.8 nM ^{R*}oligo^{*F} was added to 7.6 nM oligo$_{16c}$, and the kinetic data were collected and analyzed. This procedure was repeated with 3.8 nM ^{R*}oligo^{*F} and 11.4 nM oligo$_{16c}$. Next, 11.4 nM oligo$_{16c}$ was incubated with 3.8 nM ^{0}oligo^{0} for 45 min to essentially complete hybridization. To this solution was added 3.8 nM ^{R*}oligo^{*F}, and the kinetic data were acquired and analyzed and the reaction rate was compared to those of the initial two reactions. The following four comparisons of reaction rates and rate constants were then made using M13mp18(+):

(1) 2.8 nM ^{R*}oligo^{*F} + 8.4 nM M13mp18, target:probe = 3:1

(2) 2.8 nM ^{R*}oligo^{*F} + (8.4 nM M13mp18 + 2.8 nM ^{0}oligo^{0}), target:probe = 2:1

(3) 2.8 nM ^{R*}oligo^{*F} + 5.6 nM M13mp18, target:probe = 2:1

(4) 2.8 nM ^{R*}oligo^{*F} + (11.2 nM M13mp18 + 5.6 nM ^{0}oligo^{0}), target:probe = 2:1

The purpose of experiment (2) primarily was to demonstrate the successful blocking of the target site by ^{0}oligo^{0}, which would be reflected by a decrease in the binding rate relative to (1) by 33%. In (4), the target concentration was held *constant* relative to (3), and the number of nonproductive nucleation sites was *increased* 2×.

Data Analysis for Hybridization Kinetics. The scan of ^{R*}oligo^{*F} contained two peaks, the fluorescein peak at 520 nm and the x-rhodamine peak at 612 nm (the x-rhodamine peak shifted slightly on binding, from 608 to 612 nm). The emission centered at 520 nm resulted from the fluorescence of fluorescein following absorption of the exciting 488 nm light. The x-rhodamine emission centered at 612 nm arose from two sources: emission following resonance energy transfer from fluorescein to x-rhodamine, and emission following the direct absorption of the exciting 488 nm light by x-rhodamine. The latter contribution to the x-rhodamine emission was essentially negligible, but was included in the data analysis. Considering that the 520 and 612 nm emissions derived from these three sources, it can be shown that f, the fraction of ^{R*}oligo^{*F} hybridized, is a function of the initial and final values of the x-rhodamine emission peak and also of the initial and final values of the fluorescein/x-rhodamine peak ratio. If I is emission intensity, ϱ is the ratio of the fluorescein/x-rhodamine peaks, and the superscripts 0 and F indicate initial and final values, respectively, then

$$f = \sigma(Y)/[1 - Y(1 - \sigma)] \quad (6)$$

where

$$\sigma = I^{0}_{612nm}/I^{F}_{612nm} \quad (7)$$

$$Y = (\langle\varrho\rangle - \varrho^{0})/(\varrho^{F} - \varrho^{0}) \quad (8)$$

and $\langle\varrho\rangle$ is an intermediate value of ϱ observed during the hybridization. The value of f was calculated for each of the series of scans collected after the addition of ^{R*}oligo^{*F} to either oligo$_{16c}$ or M13mp18(+) until hybridization was complete. A second-order plot, ln[(free target)/(free probe)] vs time, was constructed, the data were fit by linear regression, and the second-order rate constant, k, was calculated from the slope. The error reported is the standard error of the mean based on five separate hybridization experiments.

Kinetics of Oligo^{*F} Binding to The Complement. The emission intensity of fluorescein on the single-labeled oligomer was used to monitor the hybridization reaction as oligo^{*F} bound to the 16-mer complement, since the fluorescein in the duplex structure had approximately one-half the emission intensity of that in the single strand. Fifteen microliters of a solution of oligo^{*F} was added, to a final concentration of 2.5 nM, to 250 μL of a solution 7.5 nM in oligo$_{16c}$. Scans were taken from 500 to 550 nm every 0.5−2 min for 12.5 min and then every 2.5−5 min for 35 min. Several scans were taken after 1.5 h to ensure that an end point had been reached. The fraction of probe bound was defined as $(F^{0} - F_{i})/(F^{0} - F^{F})$, where F^{0} and F^{F} are the initial and final emission intensities, respectively, and F_{i} is the intensity at each intermediate time point. The data were fit according to a second-order kinetics plot as described earlier.

RESULTS

The labeled oligomers were very stable, both alone and in duplex structures, in terms of their fluorescein/x-rhodamine peak ratios and emission intensities; the solutions could be left at 20 °C in the dark for up to a week with little change in either. We could find no indication that aggregation of the labeled oligomer was occurring; the absorption spectra of ^{R*}oligo^{*F}, oligo^{*F}, and ^{R*}oligo showed no evidence of exciton interaction for concentrations up to 5 μM, and the band shapes of the dyes' spectra in the single-labeled oligomers were identical to those in the double-labeled oligomer. Further, the 16-mer had no significant self-complementarity that would lead to interstrand duplex formation, with subsequent polymerization, at 20−22 °C. Mergny et al. (1994), in their studies with single-labeled oligomers, worked in the micromolar range and also report no evidence for aggregation or polymerization.

Fluorescence data on the various oligonucleotides are summarized in the cycle below. The steady-state emission intensity is proportional to $(1 - Q)\Sigma\alpha_i\tau_i$, where Q is the fraction of fluorophores that are statically quenched. In the scheme shown here, the term in brackets is $\Sigma\alpha_i\tau_i$ from the lifetime data, the term in parentheses is $1 - Q$ and the product is the relative steady-state fluorescence intensity derived from the emission peaks (A, 523 nm; B, 525 nm; C, 519 nm; D, 520 nm). The ratios of total fluorescence ($\int f(\tilde{\nu})\, d\tilde{\nu}$) were essentially the same as ratios of peak intensities.

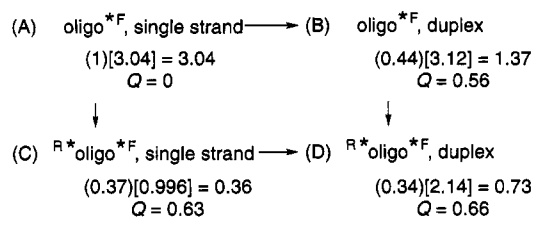

Q for species A is set equal to 0, and values for the other species are given relative to that for A. Detailed lifetime data are reported in Table 1 of the following paper in this issue (Parkhurst & Parkhurst, 1995). The ratio of the steady-state emission intensity of B/A was 0.45, and the emission maximum shifted from 523 nm for A to 525 nm for B. The fluorescence lifetime of fluorescein in A, oligo*F, was fit very well by a biexponential decay model, with $\alpha_1 = 0.75$, $\tau_1 = 3.94$ ns, $\alpha_2 = 0.25$, and $\tau_2 = 0.33$ ns. The fluorescein decay was somewhat changed, by the introduction of a second shorter lived component, from that of free fluorescein, which has a single decay of 3.95−4.0 ns. In B, oligo*F in a duplex structure, the data were also fit well by a biexponential decay model, with $\alpha_1 = 0.78$, $\tau_1 = 3.85$ ns, $\alpha_2 = 0.22$, and $\tau_2 = 0.53$ ns, which is very similar to the fluorescein decay in the single strand. The ratio of B/A of the integrated fluorescence intensities ($\sum\alpha_i\tau_i$) from the lifetime measurements was therefore 1. If Q is the fraction of fluorophores that are statically quenched, and the steady-state emission intensity is proportional to $(1 - Q)\sum\alpha_i\tau_i$, then Q for B relative to A is 0.56; we concluded that slightly over half of the fluorescein molecules were statically quenched as a result of interaction with the duplex structure and that the fluorescein decay of the molecules *not* quenched was nearly unchanged from that of the single strand. The ratio of the steady-state emission intensity of D/B was 0.53, and the ratio of their integrated intensities from lifetime measurements was 0.69; both static quenching differences and energy transfer are responsible for the difference in steady-state fluorescence emission between the two. The steady-state emission ratio of D/C, 2.0, and the ratio from lifetime integrated intensities, 2.15, were nearly identical, implying that Q must be very similar for each. That is, relative to oligo*F, approximately two-thirds of the fluorophores in R*oligo*F were statically quenched whether R*oligo*F was a single strand or in a duplex structure. In contrast, the steady-state emission ratio of C/A was 0.12, whereas the ratio of the integrated intensities of C/A was 0.33. Q for C relative to A is therefore 0.63; when x-rhodamine was bound to the 5′-end, 63% of the fluorescein emission in the single-stranded oligomer was statically quenched, apparently due to a conformational perturbation induced by the x-rhodamine and affecting the interaction of the 3′-fluorescein with the polymer. The shift in the fluorescein emission peak from 523 nm for oligo*F to 519 nm for R*oligo*F also suggests a change in conformation.

When [NaCl] was increased incrementally from 0 to 0.18 M in a solution containing oligo*F, there was no change in the fluorescein emission intensity. Q for oligo*F was therefore set equal to zero and was insensitive to [NaCl]. For R*oligo*F, the ratio of the steady-state emission in 0.18 M NaCl to that in 0 M NaCl was 0.45, and the ratio of the integrated intensities ($\sum\alpha_i\tau_i$) was 0.65. (This general departure from 1 can reflect changes in the flexibility of the oligomer and in the average distance between the fluorophores, as well as salt dependent changes in the donor emission induced by the x-rhodamine aside from energy transfer.) Relative to oligo*F, 47% of the fluorescence emission of R*oligo*F was statically quenched without NaCl, in contrast to 63% static quenching in 0.18 M NaCl. That is, increasing salt allows more interaction between the negatively charged fluorescein and polymer in R*oligo*F, whereas there are no salt dependent changes in static quenching in oligo*F.

The following observations were made with respect to the effect of 25% formamide on the fluorescein emission from labeled oligomers: The fluorescein/x-rhodamine peak ratio was 2.55 for R*oligo*F hybridized to the 16-mer complement with no formamide. In 25% formamide, for duplex structures with both $oligo_{16c}$ and M13mp18(+), the ratio was 3.1. This ratio did not change when a 100× molar excess of complement was added to the solution with the R*oligo*F/$oligo_{16c}$ duplex. For the single-stranded R*oligo*F, the fluorescein/x-rhodamine peak ratios were 0.8 and 0.5 with and without 25% formamide, respectively. When a solution of single-stranded oligo*F was made 25% in formamide, the emission intensity of the fluorescein was unchanged, but the emission doubled when oligo*F was in a duple structure. This observation was consistent with the decrease by ~2× in the fluorescein emission seen upon hybridization of oligo*F with $oligo_{16c}$ and was attributed to static quenching; apparently, the fluorescein emission was recovered because formamide interrupted the interaction of the fluorescein with the polymer. When formamide was added (to 25%) to a solution of the double-labeled oligomer, either as a single strand or in a duplex, the fluorescein emission doubled and the x-rhodamine emission increased by 40−50%. If the 2× increase in fluorescein emission were due only to the elimination of static quenching, the x-rhodamine emission would also be predicted to double. We did not further investigate the effect of formamide on these structures, but it appears from these observations that formamide may cause both the single-stranded and duplex structures to assume a more extended conformation, thus increasing ϱ. This effect may be due to increased charge repulsion along the polymer, resulting from a decrease in the dielectric constant of the aqueous buffer due to the formamide.

Hybridization Experiments and Kinetics of Hybridization. The fluorescence spectra of the double-labeled oligomer were dramatically different for the single strand and the duplex structures. The fluorescein/x-rhodamine peak ratio increased 4−5× from single strand to helix, depending on the solution conditions (Figure 2). Binding of the probe to M13mp18(+) was essentially complete, and 25−30% of the target sites in M13mp18-RF bound probe.

For the concentrations used in this study, hybridization of R*oligo*F to its 16-mer complement was complete in ~15 min without formamide and in ~20 min with 25% formamide. The ratio of the fluorescein/x-rhodamine peaks changed from 0.5 to 2.6 with no formamide and from 0.8 to 3.1 with formamide. The intensity of the fluorescencin emission doubled, and that of the x-rhodamine decreased by a factor of 2. The hybridization reaction followed second-order kinetics through at least 2 half-times; the rate constant for this reaction was $(6.4 \pm 0.22) \times 10^5$ M^{-1} s^{-1} without formamide and was slightly lower, 5.7×10^5 M^{-1} s^{-1} in each of two separate experiments, in 25% formamide.

The static quenching of fluorescein emission associated with the hybridization of oligo*F to its complement was used

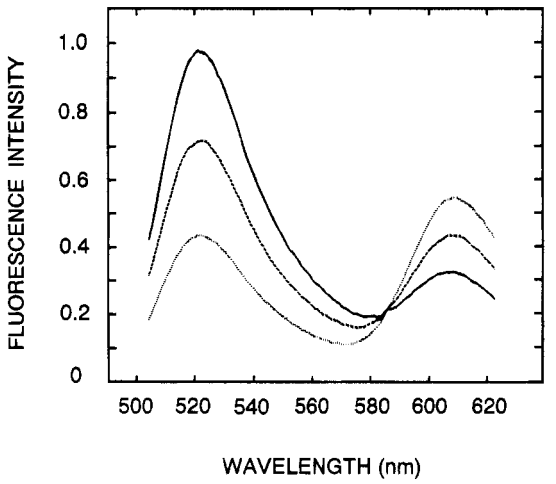

FIGURE 2: Steady-state emission scan of ^{R*}oligo^{*F}, with excitation at 488 nm, as a single strand (•••), approximately half hybridized to M13mp18(+) (- - -), and fully hybridized to M13mp18(+) (—). The buffer was 0.01 M Tris-HCl (pH 8), 1 mM EDTA, and 0.18 M NaCl, with 25% formamide. The midway scan was collected 38 min after the addition of ^{R*}oligo^{*F} to the M13mp18(+), and the final scan was taken 3 h after the addition of probe.

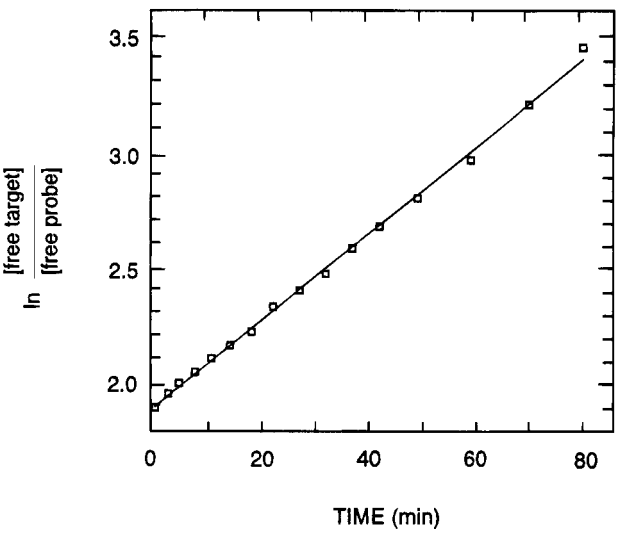

FIGURE 3: Second-order kinetic plot for the hybridization of ^{R*}oligo^{*F} to M13mp18(+), to 80% completion, showing the linear least-squares-fitted line to the observed data points. The three emission scans in Figure 2 are part of a set of 18 scans from which this plot was derived. The rate constant obtained from the slope was 6.3×10^4 M^{-1} s^{-1}.

to monitor the kinetics of that reaction. This hybridization also followed second-order kinetics, through 1.5 half-times, with a rate constant of 1×10^6 M^{-1} s^{-1}, which is faster than that measured for the double-labeled probe. (Two experiments gave values of 0.98×10^6 and 1.0×10^6 M^{-1} s^{-1}; the correlation coefficients for the regression lines were 0.997 and 0.999, respectively.) This difference is consistent with the evidence that there is significantly more interaction between the fluorescein and the polymer in ^{R*}oligo^{*F} than in oligo^{*F}, which may effectively decrease the rate at which the double-labeled probe can hybridize to its complement.

Hybridization of the ^{R*}oligo^{*F} to M13mp18(+) with no formamide was measurable but very slow, with ϱ changing by 5% in 150 min. When this solution was heated to 65 °C and cooled slowly to 20 °C, ϱ was 2.55, the same value that was obtained upon complete hybridization of the probe to its 16-mer complement. When the same solution was reheated to 65 °C, immediately cooled on ice, and then returned to ambient temperature and scanned, ϱ was 0.5, the value for the single strand, indicating melting of the duplex structure. This procedure was repeated several times, changing ϱ between 0.5 and 2.6 depending on the cooling procedure. The kinetics of hybridization of ^{R*}oligo^{*F} with M13mp18(+) was determined in 25% formamide. For the concentrations used, hybridization was complete in 120–150 min. This reaction also followed second-order kinetics, and a typical second-order plot, showing 80% of the reaction, is shown in Figure 3. The rate constant calculated for this hybridization was $(5.7 \pm 0.7) \times 10^4$ M^{-1} s^{-1}, which is one-tenth the rate constant measured for hybridization with the 16-mer complement in 25% formamide. As with hybridization of the probe to its complement in 25% formamide, $\varrho_{initial} = 0.8$, $\varrho_{final} = 3.1$, fluorescein emission intensity doubled, and x-rhodamine emission intensity decreased by a factor of 2.

When the solution of probe and double-stranded M13mp18-RF was raised to 97 °C for 2 min and cooled slowly to ambient temperature, the value of ϱ increased from 0.51 to 0.74 (with no formamide). After 24 h at 20 °C, ϱ had increased to 1.0, and it remained at that value after another 24 h at 20 °C; the probe bound ~25% of the target sites. In the control solution, ^{R*}oligo^{*F} alone, ϱ changed by <4% overall. The results in 25% formamide were similar, and kinetic data were not obtained for these reactions.

The following results were obtained in the experiments designed to differentiate between multiple nonproductive nucleation and fluctuations in structure as the source of the lower rate constant for the probe binding to M13mp18(+) compared to $oligo_{16c}$. The preliminary experiments demonstrated effective blocking of the target sequence with ^{0}oligo^0: when 11.4 nM $oligo_{16c}$ was first incubated with 3.6 nM ^{0}oligo^0 (which would be predicted to leave 7.6 nM $oligo_{16c}$ available for hybridization with the probe), the reaction rate for hybridization to 3.8 nM ^{R*}oligo^{*F} was within 10% of that measured for binding between 3.8 nM ^{R*}oligo^{*F} and 7.6 nM $oligo_{16c}$ with no ^{0}oligo^0 present and was slower by one-third than the rate for 3.8 nM ^{R*}oligo^{*F} hybridizing to 11.4 nM $oligo_{16c}$. The numbers referred to in the following statements correspond to the numbered experiments in Experimental Procedures. In 1, 2.8 nM ^{R*}oligo^{*F} was hybridized to 8.4 nM M13mp18(+). One-third of the M13mp18(+) target sites were blocked with ^{0}oligo^0 in 2, decreasing the available number of target sites to 5.6 nM, but leaving the concentration of potential nucleation sites unchanged. The reaction rate decreased by 36%, which is very close to the 33% predicted if the rate is dependent only on the target site concentration, and the rate constant calculated was 6.3×10^4 M^{-1} s^{-1}. In 3, 2.8 nM ^{R*}oligo^{*F} was hybridized to 5.6 nM M13mp18(+). Relative to 2, the target site concentration was held constant, and the number of nucleation sites was increased by one-third. The reaction rate and the calculated rate constant were within 6% of those for 2. In 4, 5.6 nM ^{0}oligo^0 was incubated with 11.2 nM M13mp18(+), leaving 5.6 nM target sites available for hybridization with 2.8 nM probe. Relative to 2 and 3, the concentration of target sites was held constant, and the number of potential nucleation sites was increased by 1.33× and 2×, respectively. The reaction rate was essentially the same as these for 2 and 3, as was the calculated rate constant,

$6.3 \times 10^4\ M^{-1}\ s^{-1}$. In summary, increasing the number of potential nucleation sites relative to the concentration of target sites up to a factor of 2 did not change the rate constant for the hybridization reaction between the probe and M13mp18(+), and there was no dependence of the rate constant on [M13mp18(+)]. These results are consistent with rapid structural fluctuations around the binding site, with an effective target site concentration 0.1 of that of the total number of sites during the reaction.

DISCUSSION

The double-labeled oligomer is very effective in signaling hybridization. Hybridization was essentially complete for the probe binding to single-stranded M13mp18(+) and could be accomplished quickly using heat followed by gradual cooling. Kinetic data were acquired in real time and did not require any further manipulation of the DNA on columns, gels, or filter paper. These rate constants are highly dependent on the solution conditions, as evidenced by the difference in rate constants determined for the simple hybridization reaction between ^{R*}oligo^{*F} and its complement, with and without 25% formamide. All hybridization reactions observed followed second-order kinetics; the second-order plot for hybridization to M13mp18(+) was linear through 80% completion, or just over 2 half-times. The results reported here differ in several respects from those reported by Gamper et al. (1987), who obtained kinetic data on a similar system using a 13-mer that was photochemically modified with HMT (furocoumarin, 4′-(hydroxymethyl)-4,5,8-trimethylpsoralen), single-stranded M13mp19, and conditions very similar to ours. The kinetics of hybridization derived from cross-linking were biphasic, which was interpreted as an initial rapid phase of probe binding to accessible target, followed by a slow phase with probe binding limited by the rate of secondary structure isomerization in the target. Maximum target coverage was 20%, which was obtained by photochemical pumping.

Our computer simulations, done in order to understand the source of the 10× decreased rate constant for ^{R*}oligo^{*F} binding to M13mp18(+), are based on two extreme models that attribute the decrease entirely to multiple nonproductive nucleation by the probe or to rapid fluctuations in structure around the target site. The simulations predict a distinct concentration dependence of the observed rate constant on [M13mp18(+)] for the multiple nucleation model and no such dependence for the model based on an inaccessible target due to structural fluctuations. Our experimental results strongly support the second model. It may be further observed that if multiple nucleations were the source of the decreased rate constant, the probe would be expected to bind M13mp18(+) *faster* in the absence of formamide than in 25% formamide, in accord with the known effect of formamide to slow hybridization kinetics; in fact, with no formamide, the probe binds too slowly for convenient measurement of the kinetics at ambient temperature. This observation also supports the conclusion that secondary or tertiary structure exists around the target site and is relaxed by formamide, rendering the target site accessible to probe.

It is clear that a significant fraction of the fluorescein is statically quenched in the labeled oligomers; our measurements therefore include information from only a part of the total fluorescein population. That population, however, is *unchanged* under our conditions for the hybridization studies with ^{R*}oligo^{*F}. The fluorescein/x-rhodamine fluorescence ratio of the double-labeled oligomer is sensitive to perturbations of fluorescein by x-rhodamine that change Q and to both the distance between the 5′ and 3′ ends and the distribution of these distances, $P(R)$ [discussed in the following paper in this issue (Parkhurst & Parkhurst, 1995)]. Changes in the value of ϱ in general can reflect subtle changes in the mean 5′−3′ distance, in the distance distribution, in static quenching (Q), and in the nontransfer perturbation of fluorescein by x-rhodamine. If only steady-state data are available, therefore, one must be very cautious in interpreting changes in the emission spectra. Because of this exquisite sensitivity, ^{R*}oligo^{*F} may prove to be a very useful tool for investigating the physical behavior of oligomers in solution.

REFERENCES

Cardullo, R. A., Agrawal, S., Flores, C., Zamecnik, P. C., & Wolf, D. E. (1988) *Proc. Natl. Acad. Sci. U.S.A. 85*, 8790−8794.

Cooper, J. P., & Hagerman, P. J. (1990) *Biochemistry 29*, 9261−9268.

Gamper, H. B., Cimino, G. D., & Hearst, J. E. (1987) *J. Mol. Biol. 197*, 349−362.

Heller, M. J., & Morrison, L. E. (1985) *Rapid Detection and Identification of Infectious Agents* (Kingsbury, D. T., & Fallow, S., Eds.) pp 245−256, Academic Press, New York.

Martin, M. M., & Lindqvist, L. (1975) *J. Lumin. 10*, 381−390.

Mergny, J.-L., Boutorine, A. S., Garestier, T., Belloc, F., Rougée, M., Bulychev, N. V., Koshkin, A. A., Bourson, J., Lebedev, A. V., Baleur, B., Thuong, N. T., & Helénè, C. (1994) *Nucleic Acids Res. 22*, 920−928.

Morrison, L. E., Halder, T. C., & Stols, L. M. (1989) *Anal. Biochem. 183*, 231−244.

Parkhurst, K. M., & Parkhurst, L. J. (1992) *Abstracts, 11th International Congress on Photobiology*, Kyoto, Japan, p 258, Photobiology Association of Japan, Kyoto, Japan.

Parkhurst, K. M., & Parkhurst, L. J. (1993) *Abstr., Biophys. J. 64*, A266.

Parkhurst, K. M., & Parkhurst, L. J. (1995) *Biochemistry 34*, 293−300.

Tenover, F. C., Ed. (1989) *DNA Probes for Infectious Disease*, CRC Press, Inc., Boca Raton, FL.

BI941622Y